European Journal of Neuroscience, Vol. 17, pp. 2201–2211, 2003

Characterization of the human visual V6 complex by functional magnetic resonance imaging

Peter Dechent and Jens Frahm
Biomedizinische NMR Forschungs GmbH am Max-Planck-Institut für biophysikalische Chemie, 37070 Göttingen, Germany

Keywords: extrastriate visual cortex, parieto-occipital sulcus, V6/V6A, visual topography, visuomotor integration

Abstract

Magnetoencephalography of a visual area along the human parieto-occipital sulcus suggested that this region represents the human homologue of the monkey visual area V6 complex (visual area V6/visuomotor area V6A) involved in the integration of visual and somatomotor information. We used functional magnetic resonance imaging at 2.0 T and $2 \times 2 \times 3\,mm^3$ resolution (16 sections) to characterize visual areas along the parieto-occipital sulcus in five healthy human subjects. Paradigms comprised a full-field checkerboard stimulation, a full-field luminance flicker as well as a foveal and peripheral luminance flicker using both a direct and differential design for comparing functional states. Along the parieto-occipital sulcus, and in contrast to primary visual areas, luminance stimulation evoked much larger activation volumes than checkerboard stimulation. Moreover, based on anatomic landmarks, luminance stimulation identified two functionally distinct regions of parieto-occipital sulcus activations: an inferior part (supposedly visual area V6) and a superior portion (supposedly visuomotor area V6A). With these assignments, foveal vs. peripheral luminance stimulation revealed a weaker foveal overrepresentation in visual area V6/visuomotor area V6A than in early visual areas, and only a mild tendency for a retinotopic organization in visual area V6. Further analyses of the functional coding of the human visual area V6 complex require functional magnetic resonance imaging at even higher spatial resolution.

Introduction

Extensive electrophysiological and immunohistochemical research in monkeys provides evidence that the successful performance of visually guided movements involves a distributed cortical network. A major candidate for integrating visual and somatomotor information and initiating successive motor output is the visual area V6 (V6) complex in the anterior bank of the parieto-occipital sulcus (POS). Its initial characterization (Gattass *et al*., 1985) and subsequent anatomic redefinition (Colby *et al*., 1988) led to a functional separation of two subregions V6 and visuomotor area V6A (V6A; Galletti *et al*., 1996). Within this framework, V6 is located in the ventral part of the anterior bank of the POS with parts extending into the posterior bank (Galletti *et al*., 1999a). It is a purely visual area characterized by motion sensitivity and a retinotopic organization of receptive fields. Emphasis on the peripheral visual field matches the lack of a foveal overrepresentation (Colby *et al*., 1988; Galletti *et al*., 1991; Galletti *et al*., 1995; Galletti *et al*., 1996; Galletti *et al*., 1999a). Complementary area V6A is located more dorsally and, in addition to motion-sensitive visual neurons without retinotopic organization, contains visually unresponsive neurons sensitive to somatomotor input (Galletti *et al*., 1993; Galletti *et al*., 1996; Galletti *et al*., 1997; Galletti *et al*., 1999b; Battaglia-Mayer *et al*., 2001; Fattori *et al*., 2001). Furthermore, V6A encompasses eye-position neurons (Nakamura *et al*., 1999) as well as neurons whose receptive fields do not change in space with gaze shift. Such 'real position' cells encode space independent of retinotopic coordinates (Galletti *et al*., 1993). Noteworthy, most of the cells in V6A respond to a combination of retina, eye and hand information (Battaglia-Mayer *et al*., 2000; Battaglia-Mayer *et al*., 2001).

The view of V6/V6A as a complex integrating visual and somatomotor information is supported by the fact that cortico-cortical inputs to V6 originate from occipital and, to a lesser extent, also from parietal areas (Shipp *et al*., 1998; Galletti *et al*., 2001). Furthermore, there are direct projections from V6 to V6A (Shipp *et al*., 1998; Galletti *et al*., 2001). Inputs into V6A originate from occipital and parietal areas as well as from reciprocal connections from portions of the premotor frontal areas (Tanné *et al*., 1995; Matelli *et al*., 1998; Shipp *et al*., 1998; Caminiti *et al*., 1999; Marconi *et al*., 2001), which most likely provide visuospatial information needed by the premotor cortex for visually guided movements. Together with the observation that cortical lesions in V6A impair visually guided arm movements (Battaglini *et al*., 2002), V6A most likely represents an early node evaluating the influence of somatomotor signals during visuomotor transformation.

In humans, functional neuroimaging using positron emission tomography (PET), functional magnetic resonance imaging (fMRI) and magnetoencephalography (MEG) demonstrated involvement of the anatomically defined homologue of the V6 complex for a variety of tasks, such as arm reaching movements (Kawashima *et al*., 1994; Grafton *et al*., 1996; De Jong *et al*., 2001a; Chapman *et al*., 2002; Simon *et al*., 2002), mental navigation (Ino *et al*., 2002), visual-based attention (Fink *et al*., 1997; Simon *et al*., 2002), eyeblinks (Hari *et al*., 1994), saccades (Jousmäki *et al*., 1996; Law *et al*., 1998) and simple visual stimulation (Vanni *et al*., 2001; Simon *et al*., 2002). A role in visuomotor integration is further strengthened by optic or visuomotor ataxia, which often involve lesions in the

Correspondence: Dr P. Dechent, as above.
E-mail: pdechen@gwdg.de

Received 29 November 2002, revised 11 March 2003, accepted 13 March 2003

doi:10.1046/j.1460-9568.2003.02645.x

POS (Perenin & Vighetto, 1988). Visual motion perception revealed prominent activations along the POS (De Jong *et al*., 1994; Dupont *et al*., 1994; Cheng *et al*., 1995; Brandt *et al*., 1998; Previc *et al*., 2000; De Jong *et al*., 2001b), in particular for self-motion perception in comparison with object motion (Kleinschmidt *et al*., 2002). MEG of these visual areas reported the absence of a relative foveal magnification (Portin & Hari, 1999) and a complete lack of retinotopy (Portin *et al*., 1998; Portin & Hari, 1999; Portin *et al*., 1999; Tzelepi *et al*., 2001).

The purpose of this work was to complement recent MEG studies by an evaluation of the basic visual properties of cortical areas along the POS, the putative human V6 complex, using fMRI at improved spatial resolution. Visual stimuli included a full-field checkerboard and luminance flicker as well as a foveal and peripheral version of the luminance flicker. These choices were motivated by previous studies demonstrating reliable visual activations in both occipital cortex (Krüger *et al*., 1998; Krüger *et al*., 1999) and along the POS (Portin *et al*., 1998; Portin & Hari, 1999).

Materials and methods

Subjects

Five healthy volunteers (four females, one male; mean age 24 years, range 22–28 years) were recruited and gave informed written consent before all examinations. Procedures were approved by the Institutional Review Board.

Magnetic resonance imaging

All studies were conducted at 2.0 T (Siemens Magnetom Vision, Erlangen, Germany) using the standard headcoil. As demonstrated in Fig. 1, sagittal T1-weighted 3D gradient-echo (fast low angle shot, FLASH) images were employed to define the orientation of transverse-to-coronal sections parallel to the calcarine fissure. This section orientation was preferred because it not only allows to efficiently cover most of the visual system in the occipital and parietal lobe, but also minimizes the influence of susceptibility artefacts in the vicinity of air-filled spaces. Functional mapping was accomplished by using a blood oxygenation level-dependent

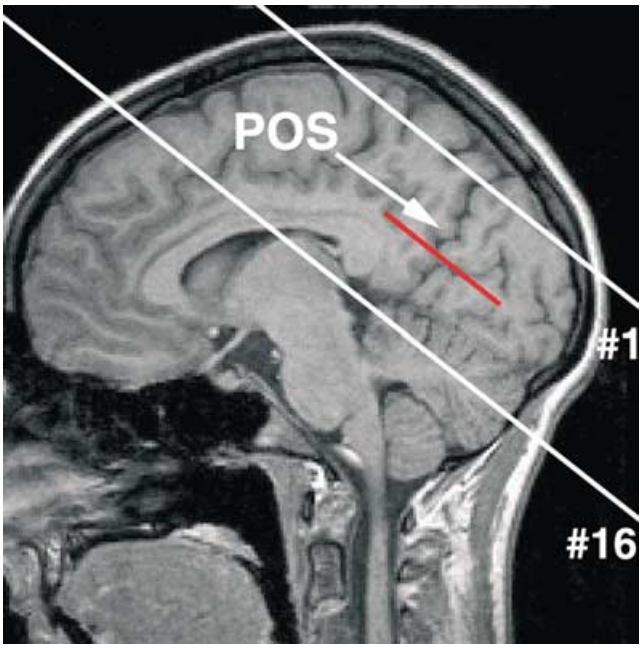

FIG. 1. Sagittal T1-weighted anatomic MR image depicting the orientation of the volume (16 sections) selected for functional mapping of the visual system including areas adjacent to the POS. The red bar represents the reconstructed plane used for dividing the POS into an inferior and superior portion (for details see text).

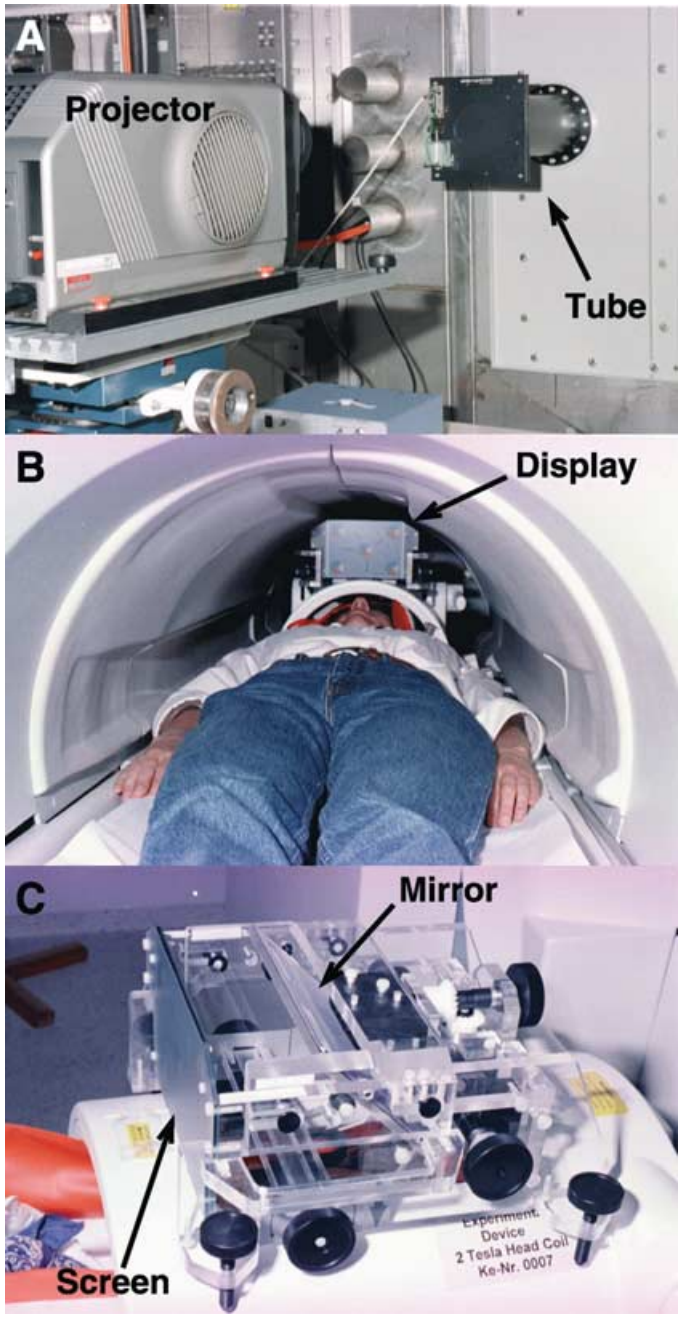

FIG. 2. Experimental setup for the presentation of visual stimuli. (A) Stimuli were generated by a computer and fed into a modified video projector. They were projected from outside the magnet room through a radiofrequency-shielded tube into (B) the magnet bore onto (C) a head-mounted translucent display atop the MRI headcoil. The subjects viewed the projected stimulus through two oculars via a 45 ° mirror. The setup covered $\pm 20^\circ \times \pm 15^\circ$ of the subjects' visual field.

echo-planar imaging sequence (repetition time 2000 ms, mean echo time 53 ms, flip angle 70 °, 16 sections) at $2 \times 2\,mm^2$ resolution and 3 mm section thickness.

Visual stimuli and paradigms

Visual stimulation was accomplished by using computer-generated stimuli projected from outside the magnet room onto a head-mounted translucent screen atop of the MRI headcoil and in front of a 45° mirror (Schäfter & Kirchhoff, Hamburg, Germany). The experimental setup is shown Fig. 2. The subjects viewed the screen through two oculars with an eye-to-screen distance of approximately 19 cm. Individual weak-sightedness was corrected by adding suitable lenses to the oculars. The setup allowed for a $\pm 20° \times \pm 15°$ coverage of the subjects' visual field in the horizontal and vertical directions, respectively. Possible light reflections during stimulation were avoided by lining the inside of the head-mounted equipment with black velvet.

The study comprised four different visual stimuli reversing black and white segments at a frequency of 5 Hz (100% luminance contrast): a radial full-field checkerboard commonly applied for activating major parts of the visual system in humans and nonhuman primates, as shown in Fig. 3A, a full-field luminance flicker as well as a foveal (<6.5° of the subjects' visual field, Fig. 3B) and peripheral version of the luminance flicker (>13°, Fig. 3C). With the used projection setup, the visual field covered by peripheral stimulation was fivefold larger than that by foveal stimulation. During the entire MRI session, the magnet room was darkened and the subjects were instructed to fixate a central cross to minimize eye movements during scanning.

Each subject underwent a total of six different functional experiments. Figure 4 sketches the two types of protocols and analysis strategies used. First, in a direct approach designed to map the cortical representations of stimulus features, each of the four above-mentioned stimuli (20 s) was contrasted with darkness (20 s). Six

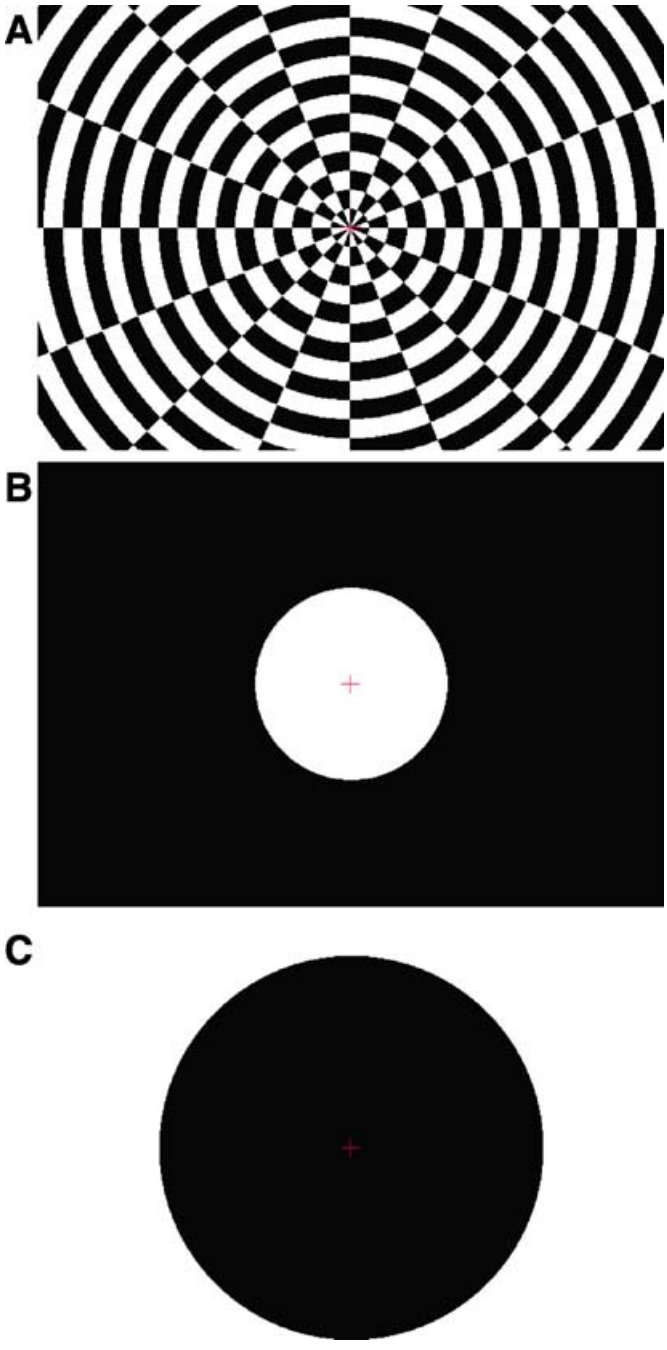

FIG. 3. Selected stimuli used for visual stimulation. (A) A radial full-field checkerboard, (B) a foveal luminance stimulus (<6.5 ° of the subjects' visual field) and (C) a peripheral luminance stimulus (>13 °). In all stimuli, black and white fields were reversing at a frequency of 5 Hz (100% luminance contrast). The subjects were instructed to fixate the central red cross to minimize eye movements.

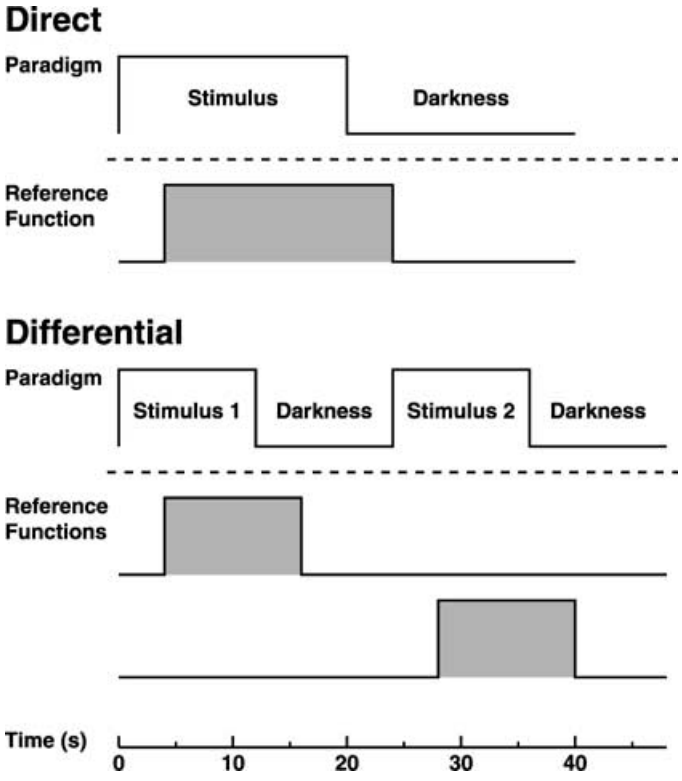

FIG. 4. Schematic drawing of stimulation paradigms and respective boxcar reference functions used for analysing direct activations (all cortical representations of a stimulus) or differential activations (areas of functional predominance of a stimulus) by cross-correlation with individual pixel intensity time courses. Reference functions are shifted relative to stimulus onset to account for haemodynamic latencies. For details of visual stimuli see text.

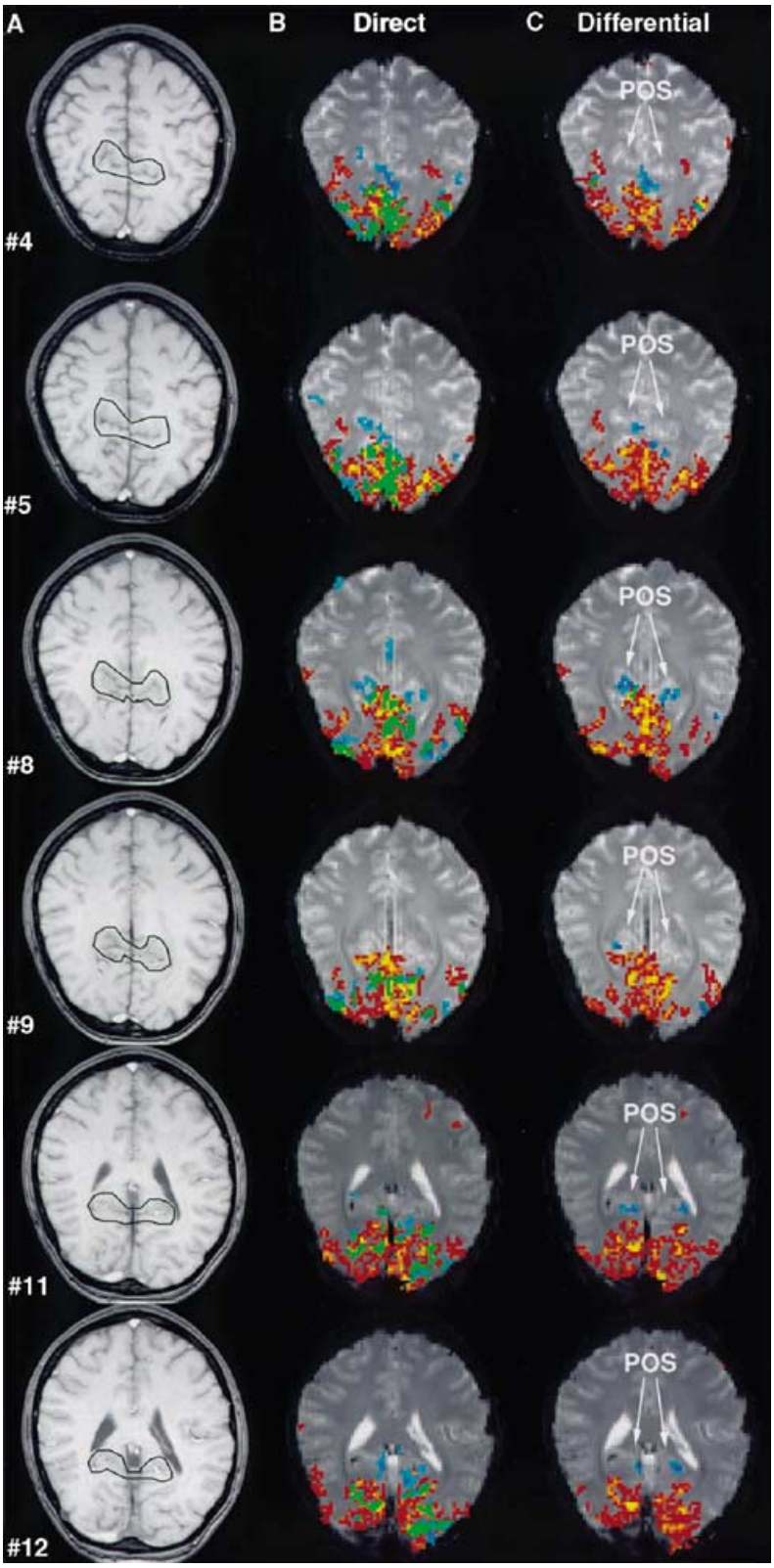
A
B Direct
C Differential
POS
#4
#5
#8
#9
#11
#12

FIG. 5.

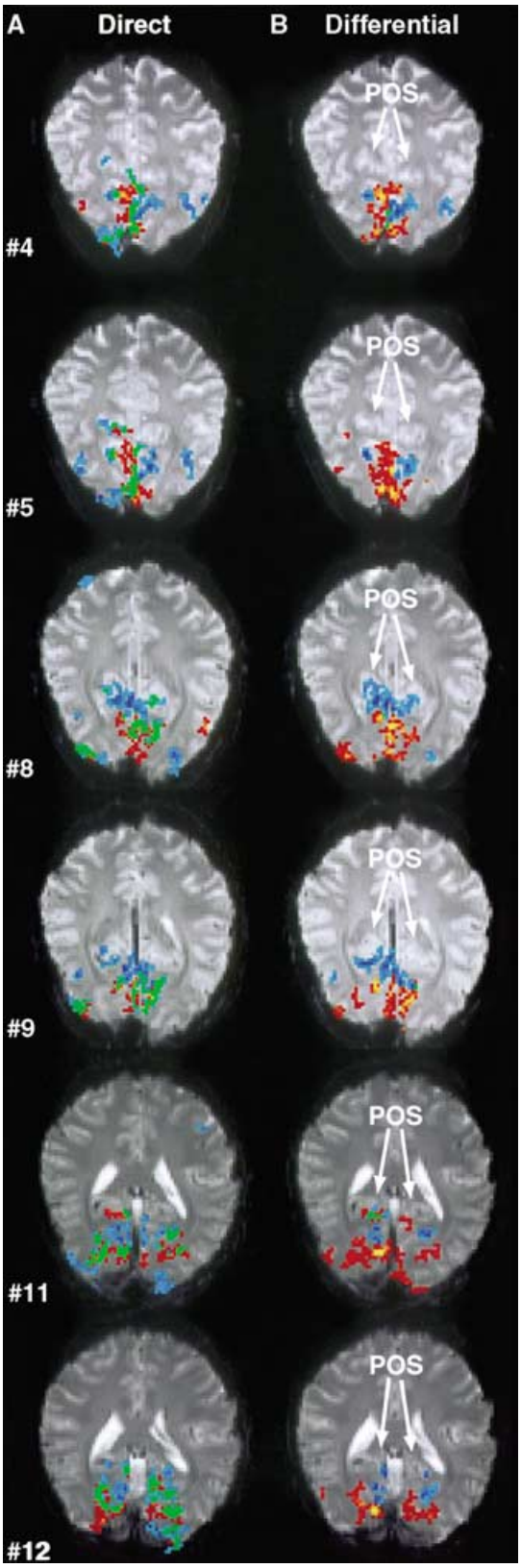
A Direct
B Differential
POS
#4
#5
#8
#9
#11
#12

FIG. 6.

repetitions resulted in a measuring time of 4 min for each of the four experiments. Second, using a differential paradigm, the full-field checkerboard (12 s) was followed by darkness (12 s) and contrasted with the full-field luminance flicker (12 s), again followed by darkness (12 s). Similarly, the foveal luminance flicker (12 s) was followed by darkness (12 s) and contrasted with the peripheral variant (12 s), again followed by darkness (12 s). Six repetitions resulted in a measuring time of approximately 5 min for each of these two experiments. The differential design highlights areas of functional predominance rather than mere cortical representations and therefore helps to identify subtle differences such as a weak retinotopic organization.

Data analysis

Three-dimensional motion correction of the fMRI data (Brain Voyager 4.7, Brain Innovation, the Netherlands) compromised the two outermost sections of the multislice data set and restricted further analyses to the 14 middle sections. Neither spatial nor temporal filtering was applied. Significantly activated pixels were identified by cross-correlation with a boxcar reference function representing changes between functional states. As indicated in Fig. 4, the analysis involved a temporal shift by two images (4 s) to account for haemodynamic latencies. This strategy further reduces putative influences from residual stimulus-correlated motions. For the four direct experiments, the reference function mimicked the protocol contrasting a particular visual stimulus (full-field checkerboard or luminance flicker, foveal or peripheral luminance flicker) with darkness. For the two differential experiments, two different reference functions analysed either predominant activations due to the first (full-field checkerboard or foveal luminance flicker) or second visual stimulus (full-field luminance flicker or peripheral luminance flicker). Activation maps were obtained by a statistical analysis using an error probability of $P \leq 0.0001$ for activation centres which were iteratively complemented by directly neighbouring pixels with $P \leq 0.05$ (adapted from Kleinschmidt *et al*., 1995). No minimum cluster size was used as a criterion for accepting activations in order to preserve the acquired high spatial resolution. To avoid inaccuracies with anatomic overlays, the activation maps were superimposed onto the original T2*-weighted functional echo-planar images.

A quantification of activated areas was performed both globally, including all visual areas within the investigated brain volume, and locally, focusing on activations along the POS. The definition of suitable regions-of-interest is indicated in the anatomic sections shown in Fig. 5A. The identification of multiple activation clusters along the POS was facilitated by projecting them into a standardized glass brain (Brain Voyager 4.7, Brain Innovation). In order to test for a putative functional segregation of activations along the POS, the junctions of the right and left calcarine fissure and the corresponding POS served as anatomic landmarks dividing the POS into an inferior and superior portion. Their mean Talairach coordinates averaged across subjects were -61.4 ± 3.3 mm (posterior–anterior, P–A direction) and 6.8 ± 4.1 mm (inferior–superior, I–S direction), as well as -64.2 ± 3.6 mm (P–A) and 5.2 ± 3.4 mm (I–S) for the right and left hemisphere, respectively. The coordinates in individual subjects were used to reconstruct a plane perpendicular to the POS, as indicated by red bars in Figs 1 and 8.

Mean locations and relative distances of activations were based on the geographical centres of individual activation clusters in terms of centre-of-mass coordinates. Such intrasubject comparisons were accomplished by a transformation of the multislice activation maps to $1 \times 1 \times 1\,\text{mm}^3$ isotropic resolution and subsequent transformation into Talairach space (Talairach & Tournoux, 1988). For multiple clusters, the centre-of-mass coordinate referred to the mean value of individual clusters weighted by their functional effect size, that is the number of activated pixels per cluster. Statistical comparisons of activation volumes were performed using the Student's *t*-test and a significance threshold of $P < 0.05$.

TABLE 1. Activation volumes for checkerboard and luminance stimulation

Region and stimulus	Volumes (mm^3) Direct[(a)]	Differential[(b)]
Visual system		
Full-field checkerboard	51084 ± 9335	41710 ± 7052
Full-field luminance	26498 ± 9889*	5345 ± 2735*
Foveal luminance	33187 ± 13057*†	18233 ± 2870
Peripheral luminance	25187 ± 5813*	13901 ± 9411
POS		
Full-field checkerboard	1693 ± 1152	1068 ± 1063
Full-field luminance	3684 ± 1993*	2925 ± 2031*
Foveal luminance	5332 ± 3718*	780 ± 956
Peripheral luminance	5252 ± 3279*†	1286 ± 980
Inferior POS (V6)		
Full-field checkerboard	1414 ± 1151	975 ± 881
Full-field luminance	2630 ± 2408	2137 ± 2336
Foveal luminance	4607 ± 3876†	441 ± 432
Peripheral luminance	4226 ± 3767	1029 ± 942
Superior POS (V6A)		
Full-field checkerboard	279 ± 356	93 ± 208
Full-field luminance	1053 ± 771	788 ± 799
Foveal luminance	752 ± 668	339 ± 716
Peripheral luminance	1026 ± 920	257 ± 309

Values are mean $\pm$ SD ($n = 5$). [(a)]Stimuli contrasted with darkness. [(b)]Full-field checkerboard contrasted with full-field luminance, foveal luminance contrasted with peripheral luminance. *$P < 0.05$ Student's *t*-test vs. full-field checkerboard stimulation. †$P < 0.05$ Student's *t*-test vs. full-field luminance flicker.

Results

As shown in Fig. 5 for a single subject, the full-field checkerboard (coded in red) activated the primary visual cortex and adjacent

FIG. 5. (A) T1-weighted anatomic MR images and (B and C) corresponding activation maps superimposed onto original T2*-weighted echo-planar images (6 out of 16 selected sections, subject S1) for (B) a direct and (C) a differential paradigm using a full-field checkerboard stimulus (yellow to red) and a full-field luminance flicker (dark to light blue) with overlapping representations coded in green. The areas in A indicate the regions-of-interest for evaluations of the POS. Whereas a reversing checkerboard yielded strong activations in large portions of the visual system, the luminance flicker was most pronounced within the POS. Yellow and dark blue represent activations with the highest statistical significance.

FIG. 6. Activation maps superimposed onto original T2*-weighted echo-planar images (same subject S1 and sections as in Figs 5 and 7) for (A) a direct and (B) a differential paradigm using a foveal (yellow to red) and a peripheral luminance flicker (dark to light blue) with overlapping representations coded in green. In primary visual areas, differential stimulation yielded the expected retinotopic arrangement, with foveal activations in posterior locations and peripheral activations in anterior locations (e.g. compare section #9).

extrastriate areas for both the direct (Fig. 5B) and differential paradigm (Fig. 5C). On the other hand, activations elicited by the full-field luminance flicker (coded in blue) were much less pronounced in primary visual areas but involved cortical regions along the POS. In fact, the overlap (coded in green) of luminance representations with checkerboard activations obtained for a direct paradigm contrasting respective stimuli with darkness (Fig. 5B) almost vanished for a differential design yielding a complete absence of luminance representations in primary visual cortices (Fig. 5C). Figure 7 shows magnified views of the luminance data presented in Fig. 5B (coded in blue and green). The location of the POS (white lines) reveals that activations along the POS are mostly located in its posterior portion.

A quantitative analysis of activation volumes in Table 1 indicates that the cortical volume activated for the full-field luminance flicker amounts to only 52% (direct paradigm) and 13% (differential paradigm) of the volume activated by checkerboard stimulation when considering the entire investigated brain volume. In contrast, activations along the POS were considerably larger for the full-field luminance flicker than for checkerboard stimulation, yielding increases by 118% (direct paradigm) and 174% (differential paradigm), respectively. Furthermore, the representations of the full-field luminance flicker were more or less uniformly distributed along the POS, whereas checkerboard activations were preferentially located in its inferior aspect.

Activation maps for foveal and peripheral luminance stimulation are shown in Fig. 6 for both a direct and differential paradigm. Cortical representations were distributed in the occipital part of the brain with prominent activations in areas along the POS, again mainly in its posterior portion (compare with Fig. 7). A comparison of activated volumes along the POS as given in Table 1 resulted in about 44% larger activation volumes elicited by a foveal and peripheral luminance flicker than obtained for the full-field stimulus. This is despite the fact that the foveal and peripheral stimuli covered only parts of the visual field. It is noteworthy that subjects reported perceiving the spatial impression of 'moving through a tunnel' for all luminance stimulations.

Figure 8 summarizes the POS activations for a full-field luminance flicker in all subjects S1–S5. Differential colouring of activated clusters in the sagittal and transverse projections of the individual glass brain views facilitates their three-dimensional assignment. The anatomic division of cortical regions along the POS (red bars) into two subregions served to assign activation clusters to either the inferior or superior portion. Clusters with their centre-of-mass below the red bar are reported in yellow, while green clusters denote activations above the red bar. With regard to this classification, the enhanced POS activation by a foveal or peripheral luminance flicker was exclusively due to the inferior subregion, whereas no predominance of foveal or peripheral luminance stimulation was seen in the superior portion. In comparison with activations obtained for a full-field stimulus, Table 1 demonstrates that the cortical volumes activated in the inferior aspect of the POS by a foveal and peripheral luminance flicker were increased by 75% and 61%, respectively.

Because of substantial overlap of luminance representations along the POS, the use of a differential paradigm strongly reduced the activation volumes for foveal and peripheral stimulation in the inferior aspect of the POS to approximately 10% and 24% of the volumes obtained for a direct paradigm. Similar, though quantitatively less pronounced, observations apply to representations in the superior portion of the POS, which generally reveal about fourfold smaller activation volumes for luminance stimulation than in the inferior aspect. Finally, the weak checkerboard activation found along the POS mainly stems from the inferior portion, with superior contributions reduced by factors of 5 (direct paradigm) to 10 (differential paradigm).

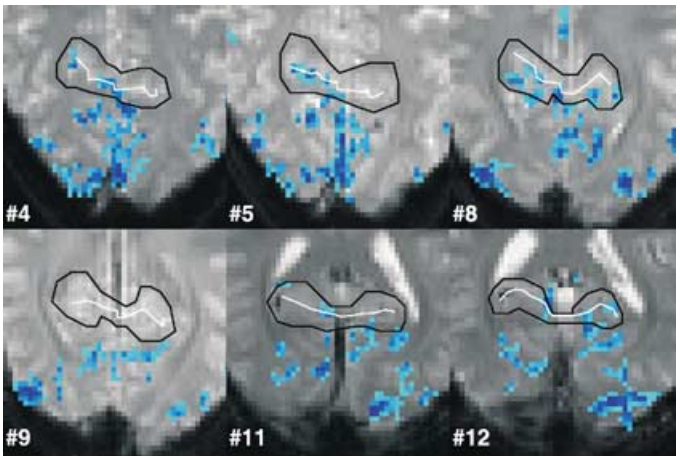

FIG. 7. Magnified views of the luminance activations shown in Fig. 5B (6 out of 16 selected sections, subject S1) for a direct paradigm and a full-field luminance flicker (dark to light blue). Apart from the regions-of-interests used for quantitative assessments (black lines), the maps indicate the location of the POS (white lines). Activations along the POS mostly occur in its posterior portion.

Table 2 presents mean centre-of-mass coordinates of cortical representations along the POS for the four different stimuli. The relative distances in the inferior aspect of the POS covered a range of 2.0 mm in the P–A direction and 2.5 mm in the I–S direction using direct paradigms, as well as 5.4 mm (P–A) and 1.4 mm (I–S) for differential paradigms, respectively. The distances in the superior portion of the POS turned out to be somewhat larger, yielding 5.8 mm (P–A) and 4.1 mm (I–S) for direct paradigms, as well as 5.0 mm (P–A) and 7.9 mm (I–S) for differential paradigms. A pictorial display of the mean coordinates for foveal (red) and peripheral (blue) luminance stimulation contrasted with darkness is shown in Fig. 9 for all subjects, and separately for the inferior and superior region. The arrows connect respective mean locations for foveal and peripheral representations in individual subjects. Whereas the inferior region reveals small distances with a consistent order across subjects, the larger distances in the superior region for three out of five subjects oppose the order found in the other two subjects.

Discussion

Representations in primary visual areas and along the POS

In comparison with strong checkerboard and weak luminance representations in primary visual areas, the situation was reversed in the areas along the POS yielding most pronounced activations in response to luminance stimulation. These findings in areas which presumably form the human visual V6 complex are in line with recent results obtained by MEG (Hari & Salmelin, 1997; Portin *et al*., 1998; Portin & Hari, 1999; Portin *et al*., 1999). They may be explained by considerable differences in the visual features of both stimuli. Because a reversing radial checkerboard provides a spatially well-defined pattern of shapes, contrast borders and orientations, which emphasizes high spatial frequencies, it is expected to strongly activate the parvocellular visual pathway known to be specialized in processing fine forms and, even though not relevant for the present study, colour. In contrast, luminance fluctuations carry only low spatial frequencies but create the

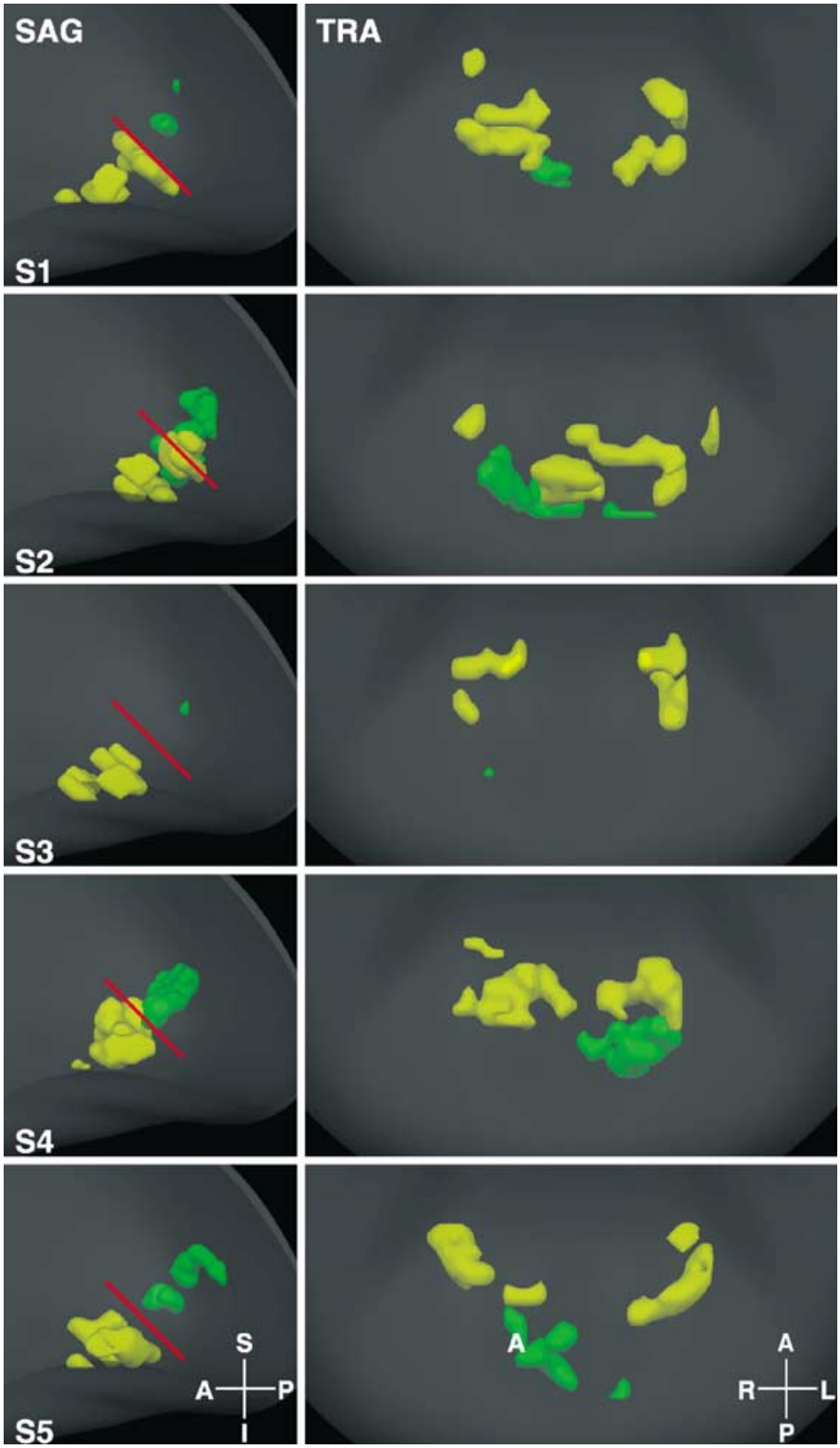

FIG. 8. Activations along the POS in response to a full-field luminance flicker contrasted with a full-field checkerboard for all subjects S1–S5. The maps correspond to sagittal (left) and transverse projections (right) of a glass brain view with coloured activations to facilitate their identification in three dimensions (A, anterior; I, inferior; L, left; P, posterior; R, right; S, superior). Whereas the hemispheric distribution of activations was rather uniform, the patterns revealed a segregation of activations into an I–A (yellow) and a S–P cluster (green), which follows individual anatomic borders (red bars).

TABLE 2. Talairach coordinates of visual representations along the POS

	Centre-of-mass coordinates in mm			
	Direct[a]		Differential[b]	
Region and stimulus	P–A	I–S	P–A	I–S
V6				
Full-field checkerboard	−58.3 ± 2.5	2.1 ± 2.3	−61.1 ± 5.2	2.5 ± 1.6
Full-field luminance	−56.8 ± 6.9	0.3 ± 2.8	−57.1 ± 5.3	1.1 ± 2.5
Foveal luminance	−57.9 ± 6.9	2.8 ± 3.8	−58.5 ± 5.5 (4)	1.1 ± 3.1 (4)
Peripheral luminance	−58.8 ± 6.0	1.5 ± 3.4	−62.5 ± 4.5 (4)	1.1 ± 2.6 (4)
V6A				
Full-field checkerboard	−72.7 ± 3.8 (3)	16.7 ± 1.6 (3)	−73.1 (1)	19.0 (1)
Full-field luminance	−69.8 ± 7.5	14.2 ± 3.1	−68.1 ± 5.9	11.7 ± 2.6
Foveal luminance	−69.5 ± 7.0	15.3 ± 3.9	−69.8 ± 0.5 (2)	16.6 ± 2.9 (2)
Peripheral luminance	−66.9 ± 7.3	12.6 ± 6.2	−68.1 ± 5.9 (4)	11.1 ± 3.2 (4)

Values are mean coordinates ± SD ($n = 5$ unless otherwise stated in parentheses) in a P–A and I–S orientation, with larger values corresponding to more anterior and more superior locations, respectively. [a]Stimuli contrasted with darkness. [b]Full-field checkerboard contrasted with full-field luminance, foveal luminance contrasted with peripheral luminance. Numbers (1–4) in parentheses indicate the numbers of subjects in cases when not all five subjects revealed activation.

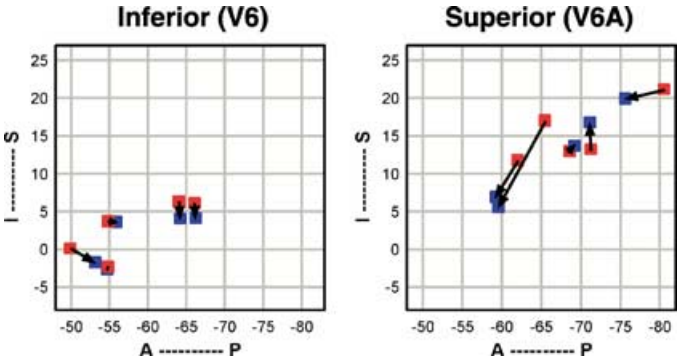

FIG. 9. Mean centre-of-mass coordinates (in mm) for the cortical representations (direct paradigm) of a foveal (red) and a peripheral luminance flicker (blue) within the POS for all subjects S1–S5 (compare with Table 2). The inferior part (V6) revealed a weak tendency for a retinotopic arrangement, that is similar directions of arrows in all subjects, not recognizable in the superior part (V6A) despite the occurrence of larger distances.

impression of motion. The luminance flicker is therefore assumed to preferentially involve the magnocellular visual pathway (Livingstone & Hubel, 1988a; for a review, see Merigan & Maunsell, 1993). Thus, the different activations found in primary visual areas may be assigned to the greater number of projections from the lateral geniculate nucleus to the primary visual cortex that belong to the parvocellular pathway as compared with the magnocellular pathway (Livingstone & Hubel, 1988b).

With regard to the quantitative predominance of luminance activations along the POS, a stimulus with a substantial degree of texture such as the radial checkerboard pattern most likely feeds the ventral 'what' stream of the visual system much stronger than the dorsal 'where' stream. Conversely, the luminance flicker gave the three-dimensional spatial impression of 'moving through a tunnel', as reported by the subjects. The underlying perception and processing of spatial information is expected to actively involve the dorsal stream of the visual system, which includes cortical areas along the POS. However, because of substantial cross-talk between the dorsal and ventral stream, processing of the stimuli used here cannot be attributed exclusively to either one of the two streams alone (for reviews, see Merigan & Maunsell, 1993; Ungerleider & Haxby, 1994).

Visual representations within V6/V6A

The functionally defined visual areas along the POS can be roughly divided into two distinct cortical regions when using the junction of the calcarine fissure and the POS as an anatomic landmark. Because these areas have been suggested to represent the human homologue of the monkey V6/V6A complex (Hari & Salmelin, 1997), and because in monkey V6 is ventrally and V6A dorsally located (Galletti *et al*., 1999a; Galletti *et al*., 1999b), the inferior portion is tentatively assigned to the human visual area V6 and the superior aspect to the visuomotor area V6A. Whereas in monkeys, areas V6 and V6A are located mostly in the anterior bank of the POS, the present observation in humans shows visual representations mainly in the posterior portion of the POS (compare with Fig. 7), as also recently reported in PET and MEG studies (Brandt *et al*., 1998; Law *et al*., 1998; De Jong *et al*., 2001b; Tzelepi *et al*., 2001; Vanni *et al*., 2001). Thus, it seems more appropriate to characterize the human visual complex along the POS as an 'analogy' rather than a 'homology' to the monkey V6 complex.

An important finding is the much stronger representation of all visual stimuli in V6 as opposed to V6A. Although it cannot be entirely excluded that minor differences in vascularization contribute to this effect, a more likely explanation would be that V6 occupies a bigger portion of cortex and thus leads to an inherently larger activated volume. However, it contradicts results from monkey studies, which give the impression that V6A is much larger than V6 (Galletti *et al*., 1999a; Galletti *et al*., 1999b). Even when taking into account possible evolutionary differences between species, one would expect the integration of visual and somatomotor information in humans to be at least as well developed as in monkeys, and thus disregard a decreased size of human V6A. A more probable possibility assumes that the visual stimuli used here are well suited for activating a purely visual area such as V6, but are less adequate for

involving visuomotor area V6A without an active motor component. This view would be in line with monkey studies reporting that, in contrast to V6 (Galletti *et al*., 1999a), only 61% of the neurons in V6A respond to mere visual stimulation (Galletti *et al*., 1999b). It is further strengthened by the fact that checkerboard stimulation caused an activated volume in V6A of only approximately 20% of that found in V6 (only 10% for a differential paradigm). On the other hand, full-field luminance stimulation with its three-dimensional motion impression yielded a V6A activation of approximately 40% of that in V6 (and still 37% for a differential paradigm). Together, these results support the existence of functionally distinct regions along the human POS with different subspecialities in visual and visuomotor processing which dominate over putative differences in the size of respective cortical areas. In order to further strengthen this view, the superior portion (supposedly the visuomotor area V6A) should specifically be tested for its responsiveness to somatomotor input, for example, by adopting stimuli from respective monkey studies (Galletti *et al*., 1997; Battaglia-Mayer *et al*., 2001; Fattori *et al*., 2001).

It is interesting to note the quantitative predominance of a foveal and peripheral luminance flicker in V6/V6A over full-field stimulation. When examining V6 and V6A separately, it turns out that the V6A cortical volumes were of similar size for all luminance stimuli, whereas in V6 the activated volume for the foveal and peripheral stimulus was almost twice as large as that for the full-field flicker. Part of the effect may be attributed to the presence of additional visual features for foveal and peripheral stimuli, such as the occurrence of contrast borders and shape information. It may be assumed that processing of such features involves additional neuronal populations in the visual area V6 without posing a higher processing load onto the visuomotor area V6A.

Retinotopy?

A comparison of foveal and peripheral luminance representations unravelled the expected retinotopic organization in early visual areas when using the more discriminative differential paradigm design (e.g. compare section #9 in Fig. 6B covering the calcarine fissure). In contrast, foveal and peripheral luminance representations along the POS exhibit substantial overlap, which is also expressed by a significant reduction of activated volumes for differential paradigms (see Table 1). Such observations suggest that a retinotopic concept is less rigorously implemented in higher visual areas such as the V6 complex. The data summarized in Table 2 and visualized for all subjects in Fig. 9 reveal only a weak tendency for an orderly arrangement of foveal vs. peripheral representations in V6 with (linear) distances of respective mean locations (in P–A and I–S directions), which turned out to be very small. This still ambiguous finding of a V6 retinotopy is somewhat in between recent human MEG studies, which failed to identify a retinotopic order, and single-cell recordings in monkeys showing a clear retinotopic arrangement in V6 (Galletti *et al*., 1999a) but not in V6A (Galletti *et al*., 1999b). Most likely, the discrepancy in V6 must be ascribed to the limited spatial resolution of functional neuroimaging methods covering large populations of neurons as opposed to electrophysiological recordings of a single cell. In addition, future examinations need to explore a more fine-scaled set of stimuli providing detailed access to the subjects' visual field representations. Under such circumstances, it may be assumed that an orderly retinotopic layout in a relatively small cortical area such as V6 will become detectable with use of specialized high-resolution fMRI techniques, such as recently applied for studying human ocular dominance columns (Dechent & Frahm, 2000) and fine-scale finger somatotopy (Dechent & Frahm, 2003).

Foveal overrepresentation?

One distinct feature of the cortical representation of retinal input, especially in early visual areas, is the relative cortical magnification of the foveal fraction of the visual field. For example, human neuroimaging showed that the central 12 ° of the visual field occupy an excessive portion of the cortex (Sereno *et al*., 1995; Engel *et al*., 1997), which weakens over successive hierarchically organized visual areas. Here, although the foveal stimulus covered a portion of the visual field which was only approximately 20% the size of the area stimulated by the peripheral luminance flicker, its cortical representation accounted for a 32% larger activated volume in the investigated brain volume. Along the POS, foveal and peripheral stimuli resulted in rather similar activation volumes in both V6 and V6A. This observation supports a foveal overrepresentation, though in a quantitatively less pronounced manner than usually found in primary visual cortex (Sereno *et al*., 1995; Engel *et al*., 1997). The finding contradicts both electrophysiological results in monkeys (Galletti *et al*., 1999a; Galletti *et al*., 1999b) and MEG findings in humans (Portin & Hari, 1999), which suggest a complete lack of foveal overrepresentation. Similar to the unresolved issue of a retinotopic organization of V6, also this question needs to be addressed with more sophisticated stimuli (Sereno *et al*., 1995; Engel *et al*., 1997).

Conclusions

Within the framework of a distributed network of occipital, parietal and frontal cortical areas subserving visually guided movements (for reviews, see Rizzolatti *et al*., 1997; Caminiti *et al*., 1998), the V6 complex, and especially V6A, is thought to represent an early node for the integration of visual and somatomotor information (Galletti *et al*., 1996; Galletti *et al*., 1997). Here, fMRI mapping of visual areas along the human POS resulted in two functionally distinct regions in a more inferior and a more superior location. A tentative assignment to human V6 and V6A, respectively, showed that V6 responded more strongly to visual features than V6A, indicating its hierarchically lower order as a pure visual area. Furthermore, the results support the notion that higher-order processing in V6A might involve features of three-dimensional space perception in line with its role in the performance of visually guided arm movements in monkeys (e.g. Fattori *et al*., 2001; Battaglini *et al*., 2002). Future studies need to address the unresolved issues of V6 retinotopy and V6/V6A foveal overrepresentation by using more dedicated stimuli and fMRI at even higher spatial resolution.

Abbreviations

FLASH, fast low angle shot; fMRI, functional magnetic resonance imaging; I–S, inferior to superior; MEG, magnetoencephalography; P–A, posterior to anterior; PET, positron emission tomography; POS, parieto-occipital sulcus; V6, visual area V6; V6A, visuomotor area V6A.

References

Battaglia-Mayer, A., Ferraina, S., Genovesio, A., Marconi, B., Squatrito, S., Molinari, M., Lacquaniti, F. & Caminiti, R. (2001) Eye hand coordination during reaching. II. An analysis of the relationships between visuomanual signals in parietal cortex and parieto–frontal association projections. *Cereb. Cortex*, **11**, 528–544.

Battaglia-Mayer, A., Ferraina, S., Mitsuda, T., Marconi, B., Genovesio, A., Onorati, P., Lacquaniti, F. & Caminiti, R. (2000) Early coding of reaching in the parietooccipital cortex. *J. Neurophysiol.*, **83**, 2374–2391.

Battaglini, P.P., Muzur, A., Galletti, C., Skrap, M., Brovelli, A. & Fattori, P. (2002) Effects of lesions to area V6A in monkeys. *Exp. Brain Res.*, **144**, 419–422.

Brandt, T., Bartenstein, P., Janek, A. & Dietrich, M. (1998) Reciprocal inhibitory visual–vestibular interaction. Visual motion stimulation deactivates the parieto-insular vestibular cortex. *Brain*, **121**, 1749–1758.

Caminiti, R., Ferraina, S. & Battaglia-Mayer, A. (1998) Visuomotor transformations: early cortical mechanisms of reaching. *Curr. Opin. Neurobiol.*, **8**, 753–761.

Caminiti, R., Genovesio, A., Marconi, B., Battaglia-Mayer, A., Onorati, P., Ferraina, S., Mitsuda, T., Gianetti, S., Squatrito, S., Maioli, M.G. & Molinari, M. (1999) Early coding of reaching: frontal and parietal association connections of parieto-occipital cortex. *Eur. J. Neurosci.*, **11**, 3339–3345.

Chapman, H., Gavrilescu, M., Wang, H., Kean, M., Egan, G. & Castiello, U. (2002) Posterior parietal cortex control of reach-to-grasp movements in humans. *Eur. J. Neurosci.*, **15**, 2037–2042.

Cheng, K., Fujita, H., Kanno, I., Miura, S. & Tanaka, K. (1995) Human cortical regions activated by wide-field visual motion: an $H_2^{15}O$ PET study. *J. Neurophysiol.*, **74**, 413–427.

Colby, C.L., Gattas, R., Olson, C.R. & Gross, C.G. (1988) Topographical organization of cortical afferents to extrastriate visual area PO in the macaque: a dual tracer study. *J. Comp. Neurol.*, **269**, 392–413.

De Jong, B.M., Shipp, S., Skidmore, B., Frackowiak, R.S.J. & Zeki, S. (1994) The cerebral activity related to the visual perception of forward motion in depth. *Brain*, **117**, 1039–1054.

De Jong, B.M., van der Graaf, F.H.C.E. & Paans, A.M.J. (2001a) Brain activation related to the representations of external space and body scheme in visuomotor control. *Neuroimage*, **14**, 1128–1135.

De Jong, B.M., van Weerden, T.W. & Haaxma, R. (2001b) Opsoclonus-induced occipital deactivation with a region-specific distribution. *Vis. Res.*, **41**, 1209–1214.

Dechent, P. & Frahm, J. (2000) Direct mapping of ocular dominance columns in human primary visual cortex. *Neuroreport*, **11**, 3247–3249.

Dechent, P. & Frahm, J. (2003) Functional somatotopy of finger representations in human primary motor cortex. *Hum. Brain Mapp.*, **18**, 272–283.

Dupont, P., Orban, G.A., de Bruyn, B., Verbruggen, A. & Mortelmans, L. (1994) Many areas in the human brain respond to visual motion. *J. Neurophysiol.*, **72**, 1420–1424.

Engel, S.A., Glover, G.H. & Wandell, B.A. (1997) Retinotopic organization in human visual cortex and the spatial precision of functional MRI. *Cereb. Cortex*, **7**, 181–192.

Fattori, P., Gamberini, M., Kutz, D.F. & Galletti, C. (2001) 'Arm reaching' neurons in the parietal area V6A of the macaque monkey. *Eur. J. Neurosci.*, **13**, 2309–2313.

Fink, G.R., Dolan, R.J., Halligan, P.W., Marshall, J.C. & Frith, C.D. (1997) Space-based and object-based visual attention: shared and specific neural domains. *Brain*, **120**, 2013–2028.

Galletti, C., Battaglini, P.P. & Fattori, P. (1991) Functional properties of neurons in the anterior bank of the parieto-occipital sulcus of the macaque monkey. *Eur. J. Neurosci.*, **3**, 452–461.

Galletti, C., Battaglini, P.P. & Fattori, P. (1993) Parietal neurons encoding spatial locations in craniotopic coordinates. *Exp. Brain Res.*, **96**, 221–229.

Galletti, C., Battaglini, P.P. & Fattori, P. (1995) Eye position influence on the parieto-occipital area PO (V6) of the macaque monkey. *Eur. J. Neurosci.*, **7**, 2486–2501.

Galletti, C., Fattori, P., Battaglini, P.P., Shipp, S. & Zeki, S. (1996) Functional demarcation of a border between areas V6 and V6A in the superior parietal gyrus of the macaque monkey. *Eur. J. Neurosci.*, **8**, 30–52.

Galletti, C., Fattori, P., Gamberini, M. & Kutz, D.F. (1999a) The cortical visual area V6: brain location and visual topography. *Eur. J. Neurosci.*, **11**, 3922–3936.

Galletti, C., Fattori, P., Kutz, D.F. & Battaglini, P.P. (1997) Arm movement-related neurons in the visual area V6A of the macaque superior parietal lobule. *Eur. J. Neurosci.*, **9**, 410–413.

Galletti, C., Fattori, P., Kutz, D.F. & Gamberini, M. (1999b) Brain location and visual topography of cortical area V6A in the macaque monkey. *Eur. J. Neurosci.*, **11**, 575–582.

Galletti, C., Gamberini, M., Kutz, D.F., Fattori, P., Luppino, G. & Matelli, M. (2001) The cortical connections of area V6: an occipito-parietal network processing visual information. *Eur. J. Neurosci.*, **13**, 1572–1588.

Gattass, R., Sousa, A.P.B. & Covey, E. (1985) Cortical visual areas of the macaque: possible substrates for pattern recognition mechanisms. In Chagas, C., Gattass, R. & Gross, C.G. (eds), Pattern Recognition Mechanisms. Pontifical Academy of Sciences, Vatican City, pp. 1–20.

Grafton, S.T., Fagg, A.H., Woods, R.P. & Arbib, M.A. (1996) Functional anatomy of pointing and grasping in humans. *Cereb. Cortex*, **6**, 226–237.

Hari, R. & Salmelin, R. (1997) Human cortical oscillations: a neuromagnetic view through the skull. *Trends Neurosci.*, **20**, 44–49.

Hari, R., Salmelin, R., Tissari, S.O., Kajola, M. & Virsu, V. (1994) Visual stability during eyeblinks. *Nature*, **367**, 121–122.

Ino, T., Inoue, Y., Kage, M., Hirose, S., Kimura, T. & Fukuyama, H. (2002) Mental navigation in humans is processed in the anterior bank of the parieto-occipital sulcus. *Neurosci. Lett.*, **322**, 182–186.

Jousmäki, V., Hämäläinen, M. & Hari, R. (1996) Magnetic source imaging during a visually guided task. *Neuroreport*, **7**, 2961–2964.

Kawashima, R., Roland, P.E. & O'Sullivan, B.T.O. (1994) Fields in human motor areas involved in preparation for reaching, actual reaching, and visuomotor learning: a positron emission tomography study. *J. Neurosci.*, **14**, 3462–3474.

Kleinschmidt, A., Requardt, M., Merboldt, K.D. & Frahm, J. (1995) On the use of temporal correlation coefficients for magnetic resonance mapping of functional brain activation: individualized thresholds and spatial response delineation. *Int. J. Imag. Syst. Technol.*, **6**, 238–244.

Kleinschmidt, A., Thilo, K.V., Büchel, C., Gresty, M.A., Bronstein, A.M. & Frackowiak, R.S.J. (2002) Neural correlates of visual-motion perception as object- or self-motion. *Neuroimage*, **16**, 873–882.

Krüger, G., Fransson, P., Merboldt, K.D. & Frahm, J. (1999) Does stimulus quality affect the physiologic MRI responses to brief visual activation? *Neuroreport*, **10**, 1277–1281.

Krüger, G., Kleinschmidt, A. & Frahm, J. (1998) Stimulus dependence of oxygenation-sensitive MRI responses to sustained visual activation. *NMR Biomed.*, **11**, 75–79.

Law, I., Svarer, C., Rostrup, E. & Paulson, O.B. (1998) Parieto-occipital cortex activation during self-generated eye movements in the dark. *Brain*, **121**, 2189–2200.

Livingstone, M. & Hubel, D. (1988a) Segregation of form, color, movement, and depth: anatomy, physiology, and perception. *Science*, **240**, 740–749.

Livingstone, M.S. & Hubel, D.H. (1988b) Do the relative mapping densities of the magno- and parvocellular systems vary with eccentricity? *J. Neurosci.*, **8**, 4334–4339.

Marconi, B., Genovesio, A., Battaglia-Mayer, A., Ferraina, S., Squatrito, S., Molinari, M., Lacquaniti, F. & Caminiti, R. (2001) Eye hand coordination during reaching. I. Anatomical relationships between parietal and frontal cortex. *Cereb. Cortex*, **11**, 513–527.

Matelli, M., Govoni, P., Galletti, C., Kutz, D.F. & Luppino, G. (1998) Superior area 6 afferents from the superior parietal lobule in the macaque monkey. *J. Comp. Neurol.*, **402**, 327–352.

Merigan, W.H. & Maunsell, J.H.R. (1993) How parallel are the primate visual pathways? *Annu. Rev. Neurosci.*, **16**, 369–402.

Nakamura, K., Chung, H.H., Graziano, M.S.A. & Gross, C.G. (1999) Dynamic representations of eye position in the parieto-occipital sulcus. *J. Neurophysiol.*, **81**, 2374–2385.

Perenin, M.-T. & Vighetto, A. (1988) Optic ataxia: a specific disruption in visuomotor mechanisms. *Brain*, **111**, 643–674.

Portin, K. & Hari, R. (1999) Human parieto-occipital visual cortex: lack of retinotopy and foveal magnification. *Proc. R. Soc. Lond.*, **266**, 981–985.

Portin, K., Salenius, S., Salmelin, R. & Hari, R. (1998) Activation of the human occipital and parietal cortex by pattern and luminance stimuli: neuromagnetic measurements. *Cereb. Cortex*, **8**, 253–260.

Portin, K., Vanni, S., Virsu, V. & Hari, R. (1999) Stronger occipital cortical activation to lower than upper visual field stimuli. *Exp. Brain Res.*, **124**, 287–294.

Previc, F.H., Liotti, M., Blakemore, C., Beer, J. & Fox, P. (2000) Functional imaging of brain areas involved in the processing of coherent and incoherent wide field-of-view visual motion. *Exp. Brain Res.*, **131**, 393–405.

Rizzolatti, G., Fogassi, L. & Gallese, V. (1997) Parietal cortex: from sight to action. *Curr. Opin. Neurobiol.*, **7**, 562–567.

Sereno, M.I., Dale, A.M., Reppas, J.B., Kwong, K.K., Belliveau, J.W., Brady, T.J., Rosen, B.R. & Tootell, R.B.H. (1995) Borders of multiple visual areas in humans revealed by functional magnetic resonance imaging. *Science*, **268**, 889–893.

Shipp, S., Blanton, M. & Zeki, S. (1998) A visuo-somatomotor pathway through superior parietal cortex in the macaque monkey: cortical connections of areas V6 and V6A. *Eur. J. Neurosci.*, **10**, 3171–3193.

Simon, O., Mangin, J.-F., Cohen, L., Le Bihan, D. & Dehaene, S. (2002) Topographical layout of hand, eye, calculation, and language-related areas in the human parietal lobe. *Neuron*, **33**, 475–487.

Talairach, P. & Tournoux, J. (1988) *A Stereotactic Coplanar Atlas of the Human Brain*. Thieme, Stuttgart.

Tanné, J., Boussaoud, D., Boyer-Zeller, N. & Rouiller, E.M. (1995) Direct visual pathways for reaching movements in the macaque monkey. *Neuroreport*, **7**, 267–272.

Tzelepi, A., Ioannides, A.A. & Poghosyan, V. (2001) Early (N70m) neuromagnetic signal topography and striate and extrastriate generators following pattern onset quadrant stimulation. *Neuroimage*, **13**, 702–718.

Ungerleider, L.G. & Haxby, J.V. (1994) 'What' and 'where' in the human brain. *Curr. Opin. Neurobiol.*, **4**, 157–165.

Vanni, S., Tanskanen, T., Seppä, M., Uutela, K. & Hari, R. (2001) Coinciding early activation of the human primary visual cortex and anteromedial cuneus. *Proc. Natl Acad. Sci. USA*, **98**, 2776–2780.